Richard C. Semelka, MD
Shahid M. Hussain, MD
Hani B. Marcos, MD
John T. Woosley, MD

Index terms:
Liver neoplasms, 761.32
Liver neoplasms, metastases, 761.332
Liver neoplasms, MR, 761.121412, 761.12143, 761.121415

Radiology 2000; 215:89–94

[1] From the Departments of Radiology (R.C.S., S.M.H., H.B.M.) and Pathology (J.T.W.), University of North Carolina Hospitals and School of Medicine, CB #7510, Chapel Hill, NC 27599-7510; and the Department of Radiology, Leiden University Medical Center, the Netherlands (S.M.H.). Received April 19, 1999; revision requested June 14; revision received June 24; accepted August 12. S.M.H. supported in part by the Dutch Cancer Society. **Address reprint requests to** R.C.S.

R.C.S. is on the speakers' bureau for Berlex and Nycomed.

Author contributions:
Guarantors of integrity of entire study, R.C.S., S.M.H.; study concepts and design, S.M.H., R.C.S.; definition of intellectual content, S.M.H., R.C.S.; literature research, S.M.H.; clinical studies, R.C.S.; data acquisition and analysis, R.C.S., S.M.H., J.T.W.; statistical analysis, S.M.H.; manuscript preparation and editing, S.M.H., R.C.S., H.B.M.; manuscript review, R.C.S.

Perilesional Enhancement of Hepatic Metastases: Correlation between MR Imaging and Histopathologic Findings—Initial Observations[1]

PURPOSE: To correlate perilesional enhancement on gadolinium-enhanced magnetic resonance (MR) images with histopathologic findings in patients with hepatic metastases.

MATERIALS AND METHODS: In seven patients with histopathologically proved hepatic metastases, MR images obtained before and early and late after the administration of gadopentetate dimeglumine were retrospectively evaluated for perilesional enhancement. The thickness of hepatic parenchyma with intense perilesional enhancement was calculated. The thickness of the histologic tumor border (the zone separating the outermost border of the tumor nodule from the surrounding hepatic parenchyma) also was measured.

RESULTS: In three patients, early gadolinium-enhanced images showed prominent perilesional enhancement, which correlated with a thick tumor border containing peritumoral desmoplastic reaction, peritumoral inflammation, and vascular proliferation at histopathologic examination. In one patient, mild perilesional enhancement was shown. At histopathologic examination, the lesion periphery showed moderate peritumoral changes. In the remaining three patients, no perilesional enhancement was observed, and at histopathologic examination there was a thin tumor border that contained minimal to mild perilesional changes. The thickness of hepatic parenchyma with intense perilesional enhancement on early gadolinium-enhanced images showed a strong positive correlation with tumor border thickness at histopathologic examination ($r = 0.99$).

CONCLUSION: Intense perilesional enhancement of metastases on early gadolinium-enhanced MR images correlates with histopathologic hepatic parenchymal changes, which include peritumoral desmoplastic reaction, inflammatory cell infiltration, and vascular proliferation.

Intense perilesional enhancement on dynamic contrast material–enhanced computed tomographic (CT) images and on magnetic resonance (MR) images acquired immediately after the administration of contrast material has been observed for a number of hepatic metastases and results in indistinct outer tumor margins and overestimation of tumor size (1,2).

Because dynamic gadolinium-enhanced MR imaging is used routinely for the evaluation and follow-up of focal hepatic lesions in many centers, the recognition and understanding of transient perilesional enhancement and its distinction from true lesional enhancement may be important for several reasons. Transient perilesional enhancement with subsequent washout on contrast-enhanced images may help to distinguish malignant from benign hepatic lesions. The determination of the exact size and location of a metastasis may be important for the planning of surgery; for the planning of minimally invasive therapy, such as cryoablation; and for the planning and follow-up of systemic chemotherapy.

To our knowledge, previous to our study, few studies have addressed the occurrence and

possible causes of perilesional enhancement on postcontrast CT and MR images (1–4). The majority of these studies (2–4) did not have histologic correlation, and the investigators in these studies postulated that the perilesional enhancement reflects the complex relationship between the dual blood supply of the liver and the local hepatic parenchymal and perfusional changes or simply correlated the findings with angiographic findings (3).

Authors of a recent study (1) correlated CT arterial portographic and equilibrium-phase postcontrast CT findings directly with histopathologic findings in 13 hepatocellular carcinomas and six hepatic metastases and described various factors that caused an overestimation of tumor size on images acquired at CT during arterial portography. To our knowledge, perilesional enhancement on dynamic, gadolinium-enhanced MR images in patients with hepatic metastases has not been correlated previously with histopathologic findings of the tumor border, which is defined as the zone separating the outermost margin of the tumor nodule from the surrounding hepatic parenchyma.

The purpose of this study was to determine the correlation of perilesional enhancement on gadolinium-enhanced MR images with histopathologic findings in patients with hepatic metastases.

MATERIALS AND METHODS

The clinical records of all patients with hepatic metastases who underwent MR imaging between August 1994 and August 1998 were cross-referenced with histopathology records in our center (the University of North Carolina Hospital). The patients were referred for an MR imaging study as their initial examination of the hepatobiliary system or as the follow-up examination of focal hepatic lesions shown on prior images.

Patients were included in the study if they met the following criteria: (*a*) having undergone resection of the hepatic metastasis and the surrounding hepatic parenchyma, (*b*) having undergone both MR imaging and surgery within 1 month, and (*c*) having undergone no intervening therapeutic intervention, including chemotherapy, between MR imaging and histopathologic examination. The clinical records of all patients were checked for evidence of chemotherapy or other treatments.

Fourteen patients met these entrance criteria; however, only seven patients had sufficient material to evaluate the tumor border well at histopathologic examination and met the inclusion criteria of our study. There were four men and three women, with an age range of 41–71 years (mean age, 56.1 years).

The hepatic metastases originated from the following primary tumors: colorectal carcinoma ($n = 5$), neuroendocrine tumor of the pancreas ($n = 1$), and transitional cell carcinoma of the bladder ($n = 1$). In one of the five patients with metastasis from colorectal carcinoma, histopathologic findings were consistent with mucinous adenocarcinoma, whereas the remaining four patients had nonmucinous adenocarcinoma.

In three patients, including two with colorectal hepatic metastases and one with metastases from neuroendocrine tumor of the pancreas, the metastatic lesions were multiple. In these patients, all lesions were nearly identical in appearance, and in each of these three patients only one lesion, the largest, was measured. The remaining four patients had solitary metastases.

MR imaging was performed with a 1.5-T MR imager (Vision; Siemens Medical Systems, Iselin, NJ). MR imaging included a T1-weighted, in-phase, breath-hold, spoiled gradient-echo sequence (repetition time of 140–175 msec and echo time of 4.1–4.5 msec [140–175/4.1–4.5]; flip angle, 80°; section thickness, 8 mm; intersection gap, 20%; one signal acquired; 21 sections in a 20-second breath hold).

Transverse spoiled gradient-echo images were acquired just prior to and immediately after intravenous bolus injection of 0.1 mmol per kilogram of body weight gadopentetate dimeglumine (Magnevist; Berlex Laboratories, Wayne, NJ), at 45 seconds, at 90 seconds with fat suppression, and at 5–10 minutes. From these five sets of images, the precontrast images, the immediately postcontrast (early) images, and the 5–10 minutes postcontrast (late) images were reviewed to determine the lesion diameter, and perilesional enhancement was determined on early postcontrast images.

One reader (S.M.H.), who was blinded to the histopathologic information and to the original MR imaging reports, retrospectively evaluated the transverse precontrast and early and late dynamic gadolinium-enhanced MR images in each patient. The retrospective MR imaging data were compared with the original MR imaging reports to determine the level of agreement for the identification of enhancement features of the metastatic lesions and of the hepatic parenchyma that surrounded the metastases.

The following features were evaluated: (*a*) intense perilesional enhancement; (*b*) the pattern of perilesional enhancement, characterized as wedge-shaped subsegmental or as circumferential perilesional enhancement; (*c*) the intensity of perilesional enhancement, as evaluated in a semiquantitative fashion with +++ meaning that perilesional enhancement was prominent, ++ meaning that it was moderate, + meaning that it was mild, -+ meaning that it was minimal, and - meaning that it was not seen; and (*d*) the longest transverse tumor diameter (in millimeters) on precontrast, early postcontrast, and late postcontrast images.

The thickness of hepatic parenchyma with intense perilesional enhancement was determined as follows: ($D_{PM} - D_{MPre} = T_{HP}$), where D is diameter, PM is enhancing perilesional tissue and metastasis, MPre is metastasis on precontrast images, and T_{HP} is the thickness of the part of the hepatic parenchyma with intense perilesional enhancement. Measurements were made on the same lesion with histologic proof, which was usually the largest lesion. Images were randomly sorted, and measurements were performed by using mechanical calipers.

The original hepatic biopsy or resection specimens were evaluated by an experienced hepatic pathologist (J.T.W.), who was blinded to the MR imaging findings. The histopathologic evaluation included the following: (*a*) evaluation of the metastasis, which included the histologic type, histologic differentiation, and the presence of fibrous stroma; (*b*) evaluation of the tumor border that surrounded the metastasis, which included peritumoral desmoplastic reaction, compressed hepatic parenchyma, atrophy of the hepatic cords, lymphocytic infiltration reflecting inflammation, vascular proliferation, indirect evidence of shunting such as the absence of fatty infiltration adjacent to the tumor in a predominantly fatty liver, vasculitis, and portal venous obstruction by tumor emboli; and (*c*) measurement of the tumor border in millimeters.

Histopathologic evaluation of the extent of the perilesional changes was performed in a semiquantitative fashion by using the following scale: A rating of +++ indicated prominent perilesional changes; ++, moderate; +, mild; −+, minimal; and −, none seen.

The Pearson correlation coefficient was calculated to compare the thickness of the intense perilesional enhancement on early gadolinium-enhanced images and the tumor border at histopathologic examination.

RESULTS

Exact agreement was observed between the retrospective and prospective readings of the extent of perilesional enhancement on immediately postcontrast images. In three of the seven patients, the lesions showed prominent perilesional enhancement, with indistinct outer tumor margins on early gadolinium-enhanced spoiled gradient-echo images (Fig 1). Approximately 20% of lesions had perilesional enhancement changes that were wedge-shaped. On late gadolinium-enhanced images, the perilesional enhancement diminished markedly or disappeared.

At histopathologic examination, the three patients' lesions were moderately differentiated adenocarcinomas, consistent with a colorectal primary carcinoma, with prominent to moderate fibrotic tumor stroma. The tumor border of these lesions showed moderate to prominent peritumoral desmoplastic reaction, mild to prominent peritumoral inflammation, minimal to mild vascular proliferation, and mild inflammatory cell infiltration (Fig 1). Compression of hepatic parenchyma and atrophy of the hepatic cords were not prominent features in these lesions.

In one of these three patients, there was minimal absence of fatty infiltration adjacent to the tumor, which may be considered an indirect sign of shunting of portal blood. No evidence was found of vasculitis or portal venous obstruction (tumor emboli) at histopathologic examination of the three patients' lesions with prominent peritumoral changes.

In one of the seven patients, early gadolinium-enhanced spoiled gradient-echo images showed mild perilesional enhancement and indistinct outer tumor margins. Associated wedge-shaped vascular abnormalities were not present. On late postcontrast images, the perilesional enhancement disappeared. At histopathologic examination, the lesion was moderately differentiated mucinous adenocarcinoma, consistent with a colorectal primary carcinoma, with prominent fibrotic tumor stroma. The tumor border showed moderate peritumoral desmoplastic reaction, mild compression of the surrounding hepatic parenchyma, mild atrophy of the hepatic cords, minimal inflammatory cells, and minimal vascular proliferation.

In the remaining three patients, no perilesional enhancement was observed on the early gadolinium-enhanced MR images (Fig 2). No wedge-shaped vascular abnormalities were present. At histopathologic examination, minimal tumor border changes were seen, which included minimal peritumoral desmoplastic reaction, minimal compression of hepatic parenchyma, minimal or mild atrophy of the hepatic cords, mild peritumoral inflammation, and minimal vascular proliferation. Table 1 contains comprehensive data and compares perilesional enhancement on MR images and histopathologic findings.

The thickness of hepatic parenchyma with intense perilesional enhancement on early gadolinium-enhanced images showed a strong positive correlation with the increasing thickness and the increasing cellular changes of the tumor border at histopathologic examination ($r = 0.99$) (Table 2). The hepatic parenchyma with perilesional enhancement on early gadolinium-enhanced images was systematically thicker than the histologic tumor

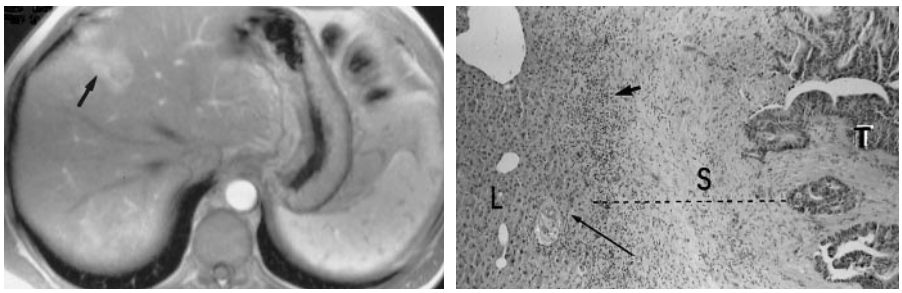

a. b.

Figure 1. Patient 2. Prominent perilesional enhancement. **(a)** Transverse, immediately postcontrast, spoiled gradient-echo (150/4.1, 80° flip angle) MR image shows intense perilesional enhancement (arrow). **(b)** Photomicrograph of the histologic specimen demonstrates prominent peritumoral desmoplastic reaction, prominent peritumoral inflammatory cell infiltration (short arrow), mild vascular proliferation (long arrow), mildly compressed hepatic parenchyma, and minimal atrophy of the hepatic cords. The nodule of metastatic, moderately differentiated adenocarcinoma (*T*) is separated from the hepatic parenchyma (*L*) by a 0.5-mm-thick zone (dashed line) of fibrocellular stroma (*S*). (Hematoxylin-eosin stain; original magnification, ×100.)

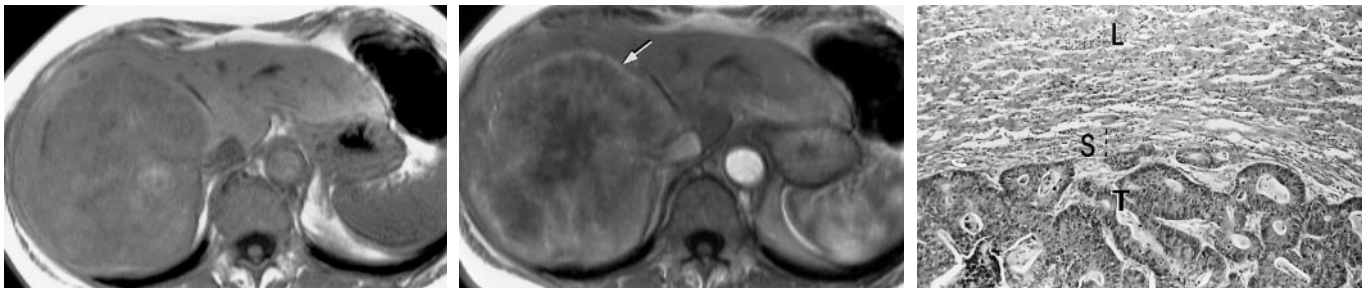

a. b. c.

Figure 2. Patient 5. No perilesional enhancement. **(a)** Transverse, precontrast, spoiled gradient-echo (150/4.1, 80° flip angle) MR image demonstrates a large metastasis in the right lobe of the liver. **(b)** Transverse, immediately postcontrast, spoiled gradient-echo (150/4.1, 80° flip angle) MR image shows no perilesional enhancement and a sharp, external border to the metastasis (arrow). The lesion diameter is identical to that in **a**. **(c)** Photomicrograph of the histologic specimen demonstrates no peritumoral desmoplastic reaction, mild peritumoral inflammatory cell infiltration, minimal vascular proliferation, minimally compressed hepatic parenchyma, and minimal atrophy of the hepatic cords. The nodule of metastatic, moderately differentiated adenocarcinoma (*T*) is separated from the surrounding hepatic parenchyma (*L*) by a 0.1-mm-thick zone (dashed line) of fibrocellular stroma (*S*). (Hematoxylin-eosin stain; original magnification, ×100.)

TABLE 1
Evaluation of Perilesional Enhancement at Histopathologic Examination

Patient No.	MR Image: Perilesional Enhancement	Histopathologic Findings: Peritumoral Desmoplastic Reaction	Compression of Hepatic Parenchyma	Atrophy of Hepatic Cords	Peritumoral Inflammation	Vascular Proliferation
1	+++	+++	−	−+	+++	+
2	+++	+++	+	−+	+++	+
3	+++	++	−+	−+	+	−+
4	+	++	+	+	−+	−+
5	−	−	−+	+	+	−+
6	−	−+	−+	−+	−	−
7	−	−	−	−	−	−

Note.—+++ = Prominent, ++ = moderate, + = mild, −+ = minimal, − = none. Patients 1–5 had metastases from colorectal carcinomas, including a mucinous type (patient 4); patient 6 had a metastasis from a transitional cell carcinoma; and patient 7 had a metastasis from a neuroendocrine pancreatic tumor.

TABLE 2
Long-Axis Tumor Diameter on MR Images

Patient No.	Long-Axis Tumor Diameter on MR Images (mm): Precontrast	Early Postcontrast	Late Postcontrast	Difference in Diameters on Early Postcontrast and Precontrast Images	Difference in Diameters on Late Postcontrast and Precontrast Images	Tumor Border Thickness at Histopathologic Examination (mm)
1	35	48	36	13	1	0.6
2	51	62	52	11	1	0.5
3	50	60	48	10	−2	0.5
4	41	44	42	3	1	0.2
5	119	121	120	2	1	0.1
6	38	39	38	1	0	0.1
7	11	11	11	0	0	0

Note.—The larger the difference in tumor diameters on early postcontrast and precontrast images, the greater the perilesional enhancement. The differences in tumor diameters on early postcontrast and precontrast images showed a high correlation with the tumor border measurements ($r = 0.99$).

Patients 1–5 had metastases from colorectal carcinomas, including a mucinous type (patient 4); patient 6 had a metastasis from a transitional cell carcinoma; and patient 7 had a metastasis from a neuroendocrine pancreatic tumor.

border in all patients. The increased enhancement on MR images was therefore not confined to the tumor border. The size of the lesions was unrelated to the extent of perilesional changes at histopathologic examination ($r = 0.10$).

In two of the seven patients with colorectal metastases (Table 1, patients 3 and 5), systemic chemotherapy was administered prior to MR imaging (but not between MR imaging and histologic assessment), which may have contributed to variable findings at MR imaging and at histopathologic examination. In one of these two patients, a decrease in perilesional enhancement was observed from prechemotherapy to postchemotherapy images (Fig 3).

DISCUSSION

Results of previous studies (2) in which immediately postcontrast images were used have shown perilesional enhancement that surrounded certain metastases. The hepatic metastases most commonly associated with this appearance have been from colorectal carcinomas (2). In our study, all patients with intense perilesional enhancement had colon cancer.

Authors of prior studies that employed CT examinations correlated the peritumoral hepatic parenchymal changes in hepatocellular carcinomas and in hepatic metastases with histopathologic findings (1,5). By using a microvascular injection technique, Lin et al (5) demonstrated compressed hepatic sinusoids that formed an avascular zone in the liver adjacent to four of 15 metastases.

More recently, Kanematsu et al (1) assessed the overestimation of the size of the hepatic malignancy at CT during arterial portography and compared the findings to the findings of equilibrium-phase CT and histopathologic examination. In that study, the CT findings of 19 resected tumors in 16 patients (13 patients with hepatocellular carcinomas and three with hepatic metastases) were directly compared with histopathologic findings (1). At histopathologic examination, the perilesional enhancement correlated with flattening of parenchymal structures, sinusoidal congestion, fibrosis, and ductular proliferation (1). Similar to the histopathologic examination in that study, the histopathologic examination in our patients with intense perilesional enhancement on early gadolinium-enhanced images showed a close correlation with peritumoral desmoplastic reaction, with peritumoral inflammatory cell infiltrates such as eosinophils and lymphocytes, and with vascular proliferation.

Investigators in previous MR imaging studies correlated the findings of T1- and T2-weighted MR imaging and histopathologic parenchymal changes in the periphery of hepatocellular carcinomas and colorectal hepatic metastases (6,7). According

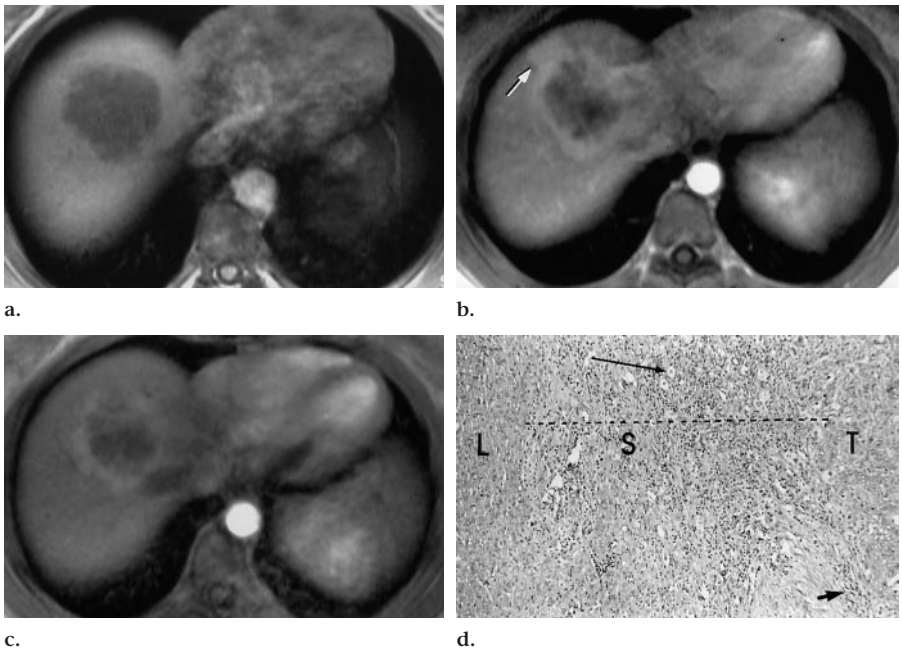

Figure 3. Patient 3. Serial changes in perilesional enhancement after systemic chemotherapy. **(a, b)** Prechemotherapy, transverse, **(a)** precontrast and **(b)** early postcontrast and **(c)** postchemotherapy, early postcontrast, spoiled gradient-echo (150/4.1, 80° flip angle) MR images. Intense perilesional enhancement (arrow in **b**) is appreciated in **b** and results in a considerable increase in lesion diameter from **a** to **b.** In **c**, after the initiation of chemotherapy, a mild decrease in intense perilesional enhancement is appreciated. **(d)** Photomicrograph of the postchemotherapy histologic specimen demonstrates moderate peritumoral desmoplastic reaction, mild peritumoral inflammatory cell infiltration (short arrow), minimal vascular proliferation (long arrow), minimally compressed hepatic parenchyma, and minimal atrophy of the hepatic cords. The nodule of metastatic, moderately differentiated adenocarcinoma (*T*) is separated from the hepatic parenchyma (*L*) by a 0.5-mm-thick zone (dashed line) of fibrocellular stroma (*S*). (Hematoxylin-eosin stain; original magnification, ×100.)

to Itoh et al (6), the inner low-signal-intensity band encompassing hepatocellular carcinomas on T2-weighted spin-echo images corresponds to the fibrous capsules, and the outer relatively high-signal-intensity area is histopathologically consistent with compressed vessels or bile duct proliferation.

Outwater et al (7) studied the morphologic patterns of colorectal hepatic metastases on T1- and T2-weighted spin-echo images in 76 patients. In 33 patients with 36 nodules, there was sufficient biopsy or resection material to yield a direct correlation between the MR imaging findings and histopathologic findings at the tumor edge and hepatic border. At histopathologic examination, 12 of 33 patients with low-signal-intensity rims around tumor nodules on the T2-weighted images showed histopathologic changes in the hepatic parenchyma adjacent to the tumor (7). The most frequent histopathologic changes included compression of hepatic parenchyma, hepatocellular atrophy, fibrosis, inflammation, and congested sinusoids (7).

The findings of the tumor border in our study confirmed the results of previous studies (1,5,6). In our study, although compressed hepatic parenchyma and atrophy of the hepatic cords were present in a majority of cases (Table 1), a combination of peritumoral desmoplastic reaction, peritumoral inflammatory cell infiltrates such as eosinophils and lymphocytes, and vascular proliferation correlated best with perilesional enhancement. Correlation between the extent of perilesional enhancement and the thickness of the tumor border was excellent; however, the thickness of the area with increased enhancement on MR images was systematically greater. Therefore, the increased perilesional enhancement was not confined to the histologic tumor border. Explanation for this difference likely includes shrinkage of the histopathologic specimen and enhancement on MR images that extends beyond the tumor border into the surrounding liver.

We presume that the inflammatory infiltrate in the tumor border increases perfusion in the adjacent zone of surrounding hepatic parenchyma by releasing local factors. The close correlation between the extent of peritumoral desmoplastic reaction and peritumoral inflammation in four of the five patients with colorectal hepatic metastases suggests that these findings may be interrelated and may result from the inherent histopathologic features of these metastases. Correlation between the perilesional hepatic parenchymal changes and the tumor grade, extent of differentiation of metastases, or their histologic type, such as mucinous or nonmucinous, would have been interesting to evaluate; however, the number of patients in our study was too small for stratification into different categories. Minimal to mild compressed hepatic parenchyma and atrophy of the hepatic cords in the majority of patients in our study may have been related to mechanical factors that resulted from tumor growth.

Several mechanisms have been proposed to explain the local increase in hepatic perfusion (3,4,8–10). These mechanisms include increased hepatic arterial flow caused by arterialization of a zone deprived of portal venous flow secondary to tumor occlusion; increased hepatic arterial flow caused by a siphoning effect of a hypervascular tumor and tumor vessels; and compressed hepatic parenchyma caused by a large intrahepatic mass, which produces an area of hypervascularity.

In addition, on the basis of our data, the increased number of inflammatory cells in the tumor border likely induces an inflammatory response in adjacent hepatic parenchyma. A combination of these mechanisms may have been responsible for the perilesional enhancement and for the wedge-shaped regions of increased enhancement observed in some of the patients in our study. It is presumed that hepatocellular damage induced by the presence of the tumor or by excretion of tumor metabolites in the direct vicinity of the tumor may have provoked inflammation and tumor neovascularity, which also may have contributed to the perilesional enhancement seen on early gadolinium-enhanced MR images.

Two patients in this study with colorectal hepatic metastases and with variable degrees of perilesional enhancement received systemic chemotherapy. In one of these two patients, MR imaging was performed prior to and after the initiation of chemotherapy and showed an interval decrease in perilesional changes. In the second patient, however, no MR imaging was performed prior to chemotherapy; therefore, the effect of chemo-

therapy could not be assessed. Chemotherapeutic agents reduce the tumor growth rate, inflammatory changes, and tumor angiogenesis (11), all of which may contribute to a decrease in perilesional enhancement. A decrease in peritumoral enhancement during chemotherapy, as observed in one of our patients, to our knowledge has not been described previously.

We believe that one of the most important features of the observation of the thickness and intensity of both the perilesional enhancement and the enhancement of the outer layer of the tumors themselves is that they may reflect a response to therapeutic interventions such as systemic chemotherapy. That is why we routinely describe these features in our prospective MR imaging reports, as was done for the patients in this study. Nonetheless, more investigative work needs to be performed to understand the frequency of the enhancement and its relation to histopathologic findings of metastatic disease and tumor growth rates. Also of great interest is the determination of whether tumor metabolites are in part responsible for the histopathologic changes.

Our study had several limitations: the small number of patients, which reflected the requirements for hepatic histopathologic examination performed relatively concurrently with MR imaging; the need for peritumoral hepatic parenchyma in the histopathologic specimen; the lack of intervening therapy between MR imaging and surgery; and the single-institutional nature of our study.

On the basis of the small number of patients, the results should be considered initial observations that require a larger number of patients to be validated. The discrepancy between MR imaging and histopathologic findings in some of our patients may in part have been attributable to variability in histopathologic sampling. Our hospital (the University of North Carolina Hospital) is a tertiary referral center for body MR imaging, and many patients who were referred for MR imaging underwent histopathologic work-up elsewhere. Often, the histopathologic material from such patients is inaccessible.

Currently, cross-sectional imaging modalities, including CT and MR imaging, allow the diagnosis of hepatic metastases noninvasively. In many cases, patients undergo fine-needle aspiration biopsy to confirm the imaging findings. Finally, because of the introduction of systemic chemotherapy and the various minimally invasive surgical techniques, which include cryotherapy, alcohol injection, and thermal ablation, in many patients with hepatic metastases, surgical resection may not be the first choice of treatment.

In conclusion, transient perilesional enhancement surrounding hepatic metastases on early gadolinium-enhanced MR images correlates with the increased thickness of the histologic tumor border and with histopathologic hepatic parenchymal changes, which include peritumoral desmoplastic reaction, inflammatory cell infiltration, and vascular proliferation.

References

1. Kanematsu M, Hoshi H, Yamada T, et al. Overestimating the size of hepatic malignancy on helical CT during arterial portography: equilibrium phase CT and pathology. J Comput Assist Tomogr 1997; 21: 713–719.
2. Larson RE, Semelka RC, Bagley AS, Molina PL, Brown ED, Lee JKT. Hypervascular malignant liver lesions: comparison of various MR imaging pulse sequences and dynamic CT. Radiology 1994; 192:393–399.
3. Freeny PC, Marks WM. Hepatic perfusion abnormalities during CT angiography: detection and interpretation. Radiology 1986; 159:685–691.
4. Itai Y, Moss AA, Goldberg HI. Transient hepatic attenuation difference of lobar or segmental distribution detected by dynamic computed tomography. Radiology 1982; 144:835–839.
5. Lin G, Gustafson T, Hagerstrand I, Lunderquist A. CT demonstration of low density ring in liver metastasis. J Comput Assist Tomogr 1984; 8:450–452.
6. Itoh K, Nishimura K, Togashi K, et al. Hepatocellular carcinoma: MR imaging. Radiology 1987; 164:21–25.
7. Outwater E, Tomaszewski JE, Daly JM, Kressel HY. Hepatic colorectal metastases: correlation of MR imaging and pathologic appearance. Radiology 1991; 180:327–332.
8. Bookstein JJ, Cho KJ, Davis GB, Dail D. Arterioportal communications: observations and hypotheses concerning transsinusoidal and transvasal types. Radiology 1982; 142:581–590.
9. Heeney DJ, Bookstein JJ, Bell RH, Orloff MJ, Miyai K. Correlation of hepatic and portal wedge venography and manometry with histology in alcoholic cirrhosis and periportal fibrosis. Radiology 1982; 142: 591–597.
10. Matsui O, Takashima T, Kadoya M, et al. Segmental staining on hepatic arteriography as a sign of intrahepatic portal vein obstruction. Radiology 1982; 152:601–606.
11. Arisawa Y, Sutanto-Ward E, Fortunato L, Sigurdson ER. Hepatic artery dexamethasone infusion inhibits colorectal hepatic metastases: a regional antiangiogenesis therapy. Ann Surg Oncol 1995; 2:114–120.